Performance of multicorrelators GNSS interference detection algorithms for Civil Aviation

Christophe Ouzeau, Christophe Macabiau, Benoit Roturier, Mikaël Mabilleau

Performance of Multicorrelators GNSS Interference Detection Algorithms for Civil Aviation

Christophe Ouzeau (TéSA/ENAC/DTI),
Christophe Macabiau (ENAC),
Benoît Roturier (DTI),
Mikaël Mabilleau (Sofreavia/DTI).

BIOGRAPHY

Christophe OUZEAU graduated in 2005 with a master in astronomy at the Observatory of Paris. He started the same year his Ph.D. thesis on degraded modes resulting from the multi constellation use of GNSS, supported by DTI and supervised by ENAC.

Christophe MACABIAU graduated as an electronics engineer in 1992 from the ENAC in Toulouse, France. Since 1994, he has been working on the application of satellite navigation techniques to civil aviation. He received his PhD in 1997 and has been in charge of the signal processing lab of the ENAC since 2000.

Benoît ROTURIER graduated as a CNS systems engineer from Ecole Nationale de l'Aviation Civile (ENAC), Toulouse in 1985 and obtained a PhD in Electronics from Institut National Polytechnique de Toulouse in 1995. He was successively in charge of Instrument Landing Systems at DGAC/STNA (Direction Générale de l'Aviation Civile/Service Technique de la Navigation Aérienne), then of research activities on CNS systems at ENAC. He is since 2000 head of GNSS Navigation subdivision at DGAC/DTI (Direction de la Technique et de l'Innovation, formerly known as STNA) and is involved in the development of civil aviation applications based on GPS/ABAS, EGNOS and GALILEO. He is also currently involved in standardization activities on future multi constellation GNSS receivers within Eurocae WG62 and is the chairman of the technical group of ICAO Navigation Systems Panel.

Mikaël Mabilleau graduated in 2006 as an electronics engineer from the Ecole Nationale de l'Aviation Civile (ENAC) in Toulouse, France. He is currently working for the French Air Navigation Service Provider (DSNA-DTI) as a consultant engineer in the GNSS Navigation domain.

ABSTRACT

For GNSS civil aviation applications, it is necessary to be able to guarantee the required level of performance specified by ICAO during a given phase of flight. The use of several GNSS components such as various signals, constellations or augmentation systems, sometimes redundant, helps monitoring the system robustness against several sources of perturbations like ionosphere or jammers for instance. In case of perturbation preventing one of the needed components to meet the phase of flight required performance, it is necessary to be able to switch to another available component in order to try to maintain if possible the level of performance in terms of continuity, integrity, availability and accuracy. But, to this end, future combined receivers must be capable of detecting the largest number of degradations that should lead to the loss of one GNSS component.

Among the perturbations, one can note atmospheric disturbances, multipath, cycle slips, interferences. It is consequently necessary to identify and test degradation detection means that will enable if possible the receiver to maintain the level of performance requirement during an aircraft flight. Because of the interests in civil aviation and the restrictive requirements associated, it is interesting to focus on the degradation detection during LPV phases of flight.

The interference is among the most feared events in civil aviation use of GNSS. Detection, estimation and removal remain an open issue and may affect pseudoranges measurements accuracy as well as integrity, continuity and even availability of those measurements. In literature, many different interference detection algorithms have been proposed at the front-end level of the receiver. For instance making chi-square tests at the ADC level, as in nominal conditions, the ADC bins distribution is Gaussian. Other non exhaustive means are to study the design of the receiver antenna or to make a spectral selectivity using filters. However, detection within tracking loops is not widely studied to our knowledge that is why it is an interesting investigation way that may complete other detection means, as proposed in [Bastide, 2001].

The goal of this paper is to estimate the performance of a detection algorithm of Carrier Waves and Narrow Bands interferences. The main results are missed detection probability and the non-detected tracking error induced by interferences. Indeed, those types of interferences may affect powerful GPS L1 C/A or Galileo E1 code spectrum lines and may produce Misleading Information. It is consequently important to study the effects of such interferences on different spectrum lines and with different settings, varying the amplitude and for Narrow Bands, the bandwidth of this perturbation. The detection algorithms used are based on multi correlator receiver outputs to detect the I and Q correlation distortions due to interferences.

The paper starts with the presentation of the detection technique. Performance analysis is then conducted taking into account required continuity during LPV phase of flight, to determine a threshold on the interference detection criteria (FFT of the correlator outputs). Interference missed detection probability is then estimated and finally the algorithm integrity

performances are discussed. To comply with actual conditions, as the receiver is supposed onboard a flying aircraft, tests were conducted under multipath conditions modelled with the DLR Aeronautical Channel, taking into account the ground reflection and fuselage echoes during LPV. In addition, simulations were performed under all kinds of dynamics, complying with DO 229 d specifications and interim Galileo MOPS.

The results indicate these techniques are good detection means under actual conditions, and do not require a too large number of calculations. The inclusion of the proposed algorithms before Receiver Autonomous Integrity Monitoring algorithms and combined integrity results are discussed. Further studies should provide results on the accuracy of interference estimation and repair algorithms.

INTRODUCTION

Within next years, the progressive apparition of new GNSS components is expected to improve the performances of the system in terms of integrity, continuity, accuracy and availability. With the use of future Galileo and modernized GPS signals, it is necessary to establish future combined receivers' architecture. The combination of Galileo and GPS signals, with possible augmentations like SBAS, ground stations or RAIM algorithms is promising for civil aviation purposes. In case of loss of one component (frequency, constellation), it should be easier to guarantee the system robustness against perturbations like multipath, ionosphere and jammers.

To do this, it is necessary to be able to detect degradations leading to a loss of performance as specified by International Civil Aviation Organization for all phases of flight and in particular for approach phases.

Several types of degradations due to various physical phenomena are identified. There is a need to define precisely the detection means that will enable the monitoring of GNSS signals used for the nominal, alternate or degraded mode, and also to switch from one mode to another one if necessary. These detection means can be located at front-end level, within tracking loops or based on pseudorange and integrity information for instance. To be accepted, those detection means have to be tested against the level of performance required for a targeted phase of flight.

Among all perturbations, it is of interest to study the effects of interferences as they can affect simultaneously several GNSS measurements. Consequently, one of the challenges for civil aviation community is to develop jamming errors detection and characterization techniques. Interferences can lead to an increased noise, a bias or a loss of the pseudoranges, and thus to a degraded navigation solution.

Generally, in literature, detection is made upstream code and phase tracking loops. Indeed, at this stage, interference detection consists in monitoring the signal and detecting when it departs from noise.

We decided to implement algorithms to detect interferences using correlator outputs, and to verify if those algorithms were compliant with civil aviation requirements for APV phases of flight. Indeed, APV is a targeted phase of flight for modern operations. It has restrictive requirements compared to phases of flight like NPA.

GNSS receivers have to be compliant with ICAO requirements in terms of integrity, continuity, accuracy and availability. Interference environment includes pure carriers, narrow band and pulsed interference signals. A listing of identified interference sources was made by RTCA (SC 159, WG 6) in [DO235A, 2002], appendix B. Those sources are classified by signalling type: pulsed or continuous. Interferences masks are designed and proposed in [MOPS Galileo, 2007], and filters will be implemented within future GNSS receivers to allow removing interferences that occur out of these masks.

On going studies on the detection and removal of pulsed interference types are being conducted at RF front-end level for instance in [Raimondi, 2006]. We focus on the detection of continuous interferences at correlator output.

Amongst the potential types of continuous interferences, Carrier Wave and Narrow Band Interferences phenomena need to be detected. If possible, they have to be located, modelled and removed from the incoming signal. The frequency occupation of those interferences is low. We will first focus on interference detection of interferences with power level below the masks.

For civil aviation applications, interferences with power level below the masks will generate acceptable degradations on tracking errors. However, we feel that when these CW interferences stay near the same code spectrum lines for a certain time, the induced tracking errors can be larger than expected by the MOPS. We feel this is important for highly restrictive approach phases of flight in terms of accuracy.

I. GENERATED SIGNALS AND INTERFERENCES

Signals affected by interferences

GPS L1 C/A and Galileo E1 signals are supposed to be affected by interferences in this study.

Low carriers to noise ratio values were chosen and are recalled in the following table. They correspond to the limit of the signal quality required for tracking, assuming a -203 dB W/Hz noise power spectral density level.

	GPS L1 C/A	GALILEO E1
C/N0 (dBHz)	40.5	34.8
Received power	-164 dBW	-168 dBW
Noise level	-203 dBW	-203 dBW

Table 1 : Minimum required carrier to noise ratios for GPS and Galileo signals from [MOPS Galileo, 2007], appendix H.

Generated interferences

The power of the generated CW is chosen to be below the interference masks provided in [MOPS Galileo, 2007], for both GPS and Galileo cases for the targeted phase of flight.

The largest CW interference power used for detection tests is -155 dBW. For NB interferences, the maximum tolerable power will differ with bandwidth.

II. IMPACT OF INTERFERENCES ON THE GENERATED SIGNALS PROCESSING

In order to justify our detection algorithms described further in this document, impacts at different levels: on correlator outputs, tracking loops and code spectrum lines of the generated interferences are shown.

- **Observed influence of interferences on correlator outputs**

After being multiplied by DLL local code and PLL local carrier, the signal is separated into two channels I and Q, the first one corresponding to the multiplication by the local estimated carrier and the second one where the signal is mixed to the quadra-phase carrier.

[Bastide, 2001] or [Macabiau, 2006] provide a description of the impact of CW on the correlator outputs. We provide hereafter a short mathematical description of this impact on GPS L1 C/A in the following.

In presence of noise only, the correlator outputs are modelled as:

$$\begin{cases} I_d(n) = \frac{A}{2} R(\varepsilon_\tau - d)\cos(\varepsilon_\varphi) + n_I(n) \\ Q_d(n) = \frac{A}{2} R(\varepsilon_\tau - d)\sin(\varepsilon_\varphi) + n_Q(n) \end{cases}$$

Where:

- R is the materialized PRN code autocorrelation function,
- A is the magnitude of the received GNSS signal,
- ε_τ is the code tracking error,
- ε_φ is the carrier phase tracking error,
- d is the delay relative to the n replica or chip spacing,
- n_I and n_Q are additive noise.

When a CW interferes with the locally generated signal, an additive sinusoidal signal resulting from the correlation between the local code and the interference will appear on the I and Q correlator channels. If that additional correlation product has a time variation characterized with a frequency greater than the PLL bandwidth B_L^{PLL}, it is then filtered out.

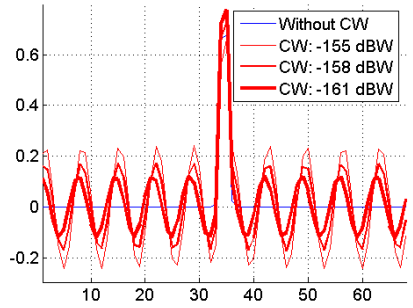

Figure 1 : Simulated correlators outputs on the I GPS L1 C/A channel affected by CW interference.

When CW interference is added to the received GNSS signal, the expressions of the correlator outputs on I and Q channels become:

$$I(n) = \frac{A}{2} D(n) R(\varepsilon_\tau)\cos(\varepsilon_\varphi) + \frac{K_J}{2}\cos(\Theta(n)) + n_I(n)$$
$$Q(n) = \frac{A}{2} D(n) R(\varepsilon_\tau)\sin(\varepsilon_\varphi) - \frac{K_J}{2}\sin(\Theta(n)) + n_Q(n)$$

$$\Theta(n) = (2\pi k_0 f_R \hat{\tau} + \varphi(n)) \quad K_J = A_J |C_{\sin c}(k_0)| \frac{\sin(\pi \delta f T_I)}{\pi \delta f T_I}$$

$$C_D(f) = \sum_{k=-\infty}^{+\infty} C_{\sin c}(k)\delta(f - k f_R)$$

$$C_{\sin c}(k) = \frac{f_R}{f_c} \frac{\sin\left(\pi k \frac{f_R}{f_c}\right)}{\pi k \frac{f_R}{f_c}} C_0(k)$$

$$\varphi(n) = 2\pi \delta f \frac{T_n}{2} - (\phi_J - \phi) + \varphi(k_0)$$

where:

- A is the amplitude of the direct GNSS signal,
- D represents the incoming signal data value during the integration interval,
- R is the materialized PRN code autocorrelation function
- $\hat{\tau}$ is the estimate of the incoming code delay,
- $\hat{\varphi}$ is the estimate of the incoming phase,
- ε_τ represents the code tracking error,
- ε_φ represents the phase tracking error,
- T_I is the integration time in seconds,
- f_R is the frequency separation between each spectral line in the local GNSS signal PSD ($f_R = \frac{fc}{CodeLength}$),
- k_0 is chosen so that $k_0 f_R$ is the frequency of the useful signal spectral line closest to f_J,
- $\delta f = k_0 f_R - f_J$,
- n_I and n_Q are the in-phase and quadra-phase correlator's output Gaussian noise assumed uncorrelated with a variance equal to $\frac{N_0}{4T_I}$
- C_0 is the discrete Fourier transform of the tracked PRN code.

We see that the correlator outputs are affected by an additive sinusoidal term, whose amplitude depends on the product of the level of the code line which is the closest to the CW by the power level of the CW interference.

In the case of a Narrow Band Interference, the interference induces a distortion which is a combination of the effect of the correlation of all the code spectrum lines with the NBI.

The same analysis can be made for Galileo E1 signal: it can be also observed a deformation of the correlation peak when interferences occur. One can mention that the correlation peak has a different shape than in the case of GPS L1 C/A signal (two secondary peaks appear beside the main one which is narrower than for GPS L1 case). In addition, the expression of $C_{\sin c}(k)$ depends upon the materialization of the signal. Indeed, in the case of Galileo E1 waveform spectrum, two main lobes will appear, centred on 1.023 MHz.

Moreover, the carrier to noise ratio can be computed at the correlator outputs to monitor the signal quality and to estimate the impact of potential interferences on the I channel prompt correlator output:

$$\left(\frac{C}{N_0}\right)_{est\_corr\_output} = \frac{1}{2T_{sampling}} \frac{mean(I)^2}{std(I)}$$

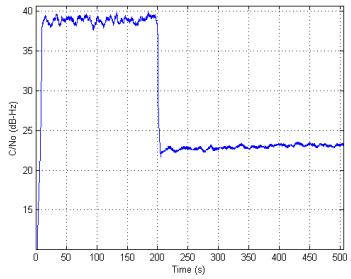

Figure 2 : C/N0 estimated without and with CW, for a generated signal 200 seconds after the beginning of the simulation.

On figure 2, carrier to noise ratio is estimated using prompt correlator output on I channel. One can see 200 seconds after the beginning of the tracking, that is to say, when the interference is generated, a loss of more than 10 dB for -155 dBW interference amplitude.

Conclusion: these observations show the interest of implementing detection algorithms based on the monitoring of these correlator outputs.

- **Code spectrum lines correlated with interference**

It is also important to consider the spectral position of the interference compared to the code spectrum lines for both GPS L1 C/A and Galileo E1 signals. In particular, the worst cases, that is to say, impacting the code spectrum lines with highest amplitudes, have to be considered to protect the user against the most penalizing interference location within signals spectra.

The additive sinusoidal term affecting the correlator outputs appears as a result of the correlation of specific code spectrum lines with the interference. Its amplitude is the product of the interference power by the code spectrum lines level. The total correlation output is the sum of the GNSS correlation peak and a $k_0 f_R$ frequency sinusoid. The higher the jammer power and the code lines magnitudes, the higher the amplitude of the sinusoid.

GPS L1 C/A and Galileo E1 code spectrum lines distributions with frequency are different; frequency spacing between Galileo code spectrum lines is narrower than for GPS. Indeed, the code period duration is four times higher for Galileo E1 than for GPS L1 C/A. It results lower amplitude of spectral lines for Galileo.

The number of spectral lines carrying the incoming signal power will influence the weight of each line. Indeed, the more spectral lines are present, the more the total incoming signal power will be distributed trough these spectral lines, and their respective weights will decrease.

As a consequence, for Galileo E1, spectrum code lines that will be impacted will be less powerful than the GPS ones. As the impact of CW on the tracking loops is expected to increase with the impacted code spectrum line amplitude, Galileo is expected to be more robust to CW interferences.

The spacing between two code spectrum lines is the code repetition frequency f_R. In case of the GPS L1 C/A code for example, the number of code spectrum lines within the main lobe of the signal power spectrum density equals twice the code length. This means that a longer code has an increased the number of lines.

The interference power driving the correlation result is the CW power in the case of a CW, and the power spectrum density in the case of NBI. For instance, the correlation of a 10 kHz Narrow Band Interference with each code spectrum line will be reduced by 40 dBW compared to a CW.

The additive sinusoidal term due to a CW on the correlation output has a phase $\Theta(n)$ which is driven in part by the frequency separation between the interference and the closest spectrum line. The choice of the PRN code spectrum lines hit by the jammer in the simulations is explained later.

The use of a secondary code, that equivalently extends the length of the spreading code, also increases the number of spectral lines and thus makes the signal less susceptible to CW/NB interference.

Worst case code spectrum lines

The worst code spectrum lines in terms of power level, for each signal are given hereafter and provided for each PRN. These power levels take into account the PRN code FFT and the Fourier transform of the materialization waveform.

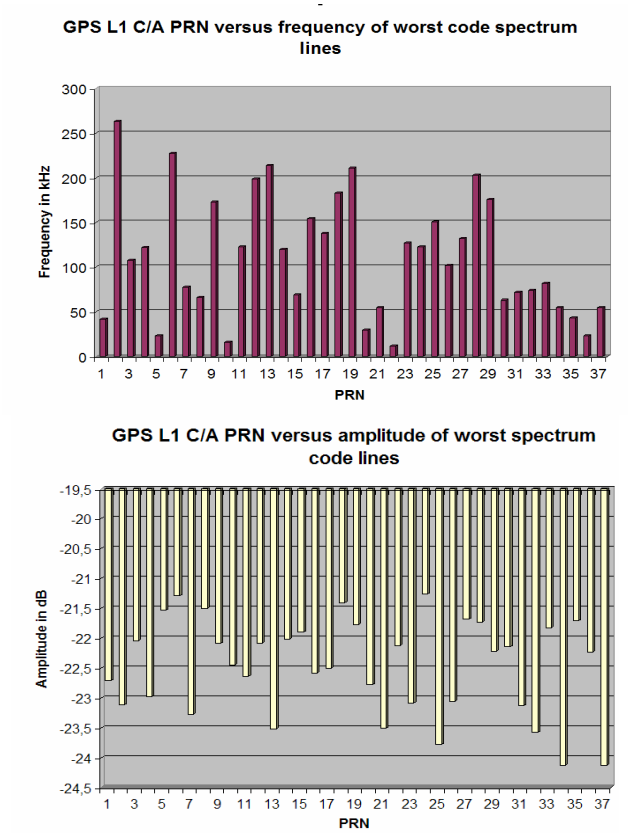

Figure 3 : GPS L1 C/A worst code spectrum lines by PRN.

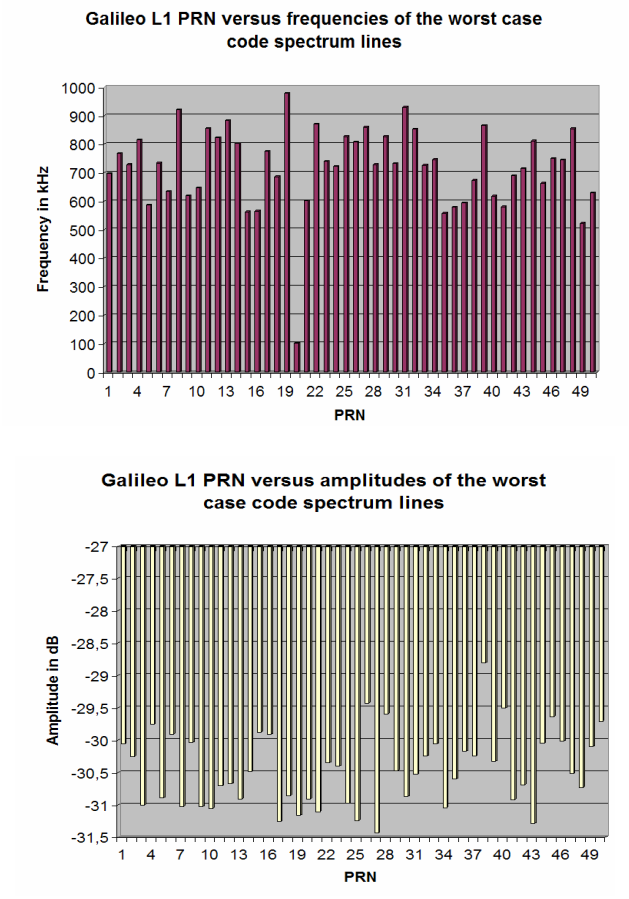

Figure 4 : Galileo E1 worst code spectrum lines by PRN.

As one can observe, for GPS L1 C/A, the worst case code spectrum line was identified on PRN 6 with a -21.29 dB level, located at a frequency of 227 kHz. For Galileo E1, the worst case code spectrum line was identified on PRN 38, located at 673.5 kHz with level -28.81 dB.

Position of the interference compared to code spectrum lines

Two important parameters can influence the spectral position and the impact of the jammer on the correlator outputs: the integration time and the residual jammer/GNSS signal Doppler. The integration time conditions the width of the weighting sinc function. A long integration time will limit the CW influence zone around each spectrum line. If the integration time was infinitely long, the CW would really have an influence only when exactly superposing with the local GNSS signal spectrum line. It is then unlikely, considering the potential Doppler residual variation between the jammer and the useful signal that such an event lasts for a very long time.

We recall hereafter integration times that we use:

Signal type	Data channel	Pilot channel
GPS L1 C/A	20 ms	4 ms
GALILEO E1	100 ms	4 ms

Table 2 : integration time of GPS and Galileo signals

NB interference will affect more code spectral lines than a CW and thus will have a greater impact on the correlator outputs.

The residual Doppler between the interference and the code spectrum lines was assumed to have a variation with time. It was set to 2 Hz per second.

- **Observed influence on tracking loops**

A 3rd order PLL with 10 Hz bandwidth and a 1st order DLL with 1 Hz bandwidth will be used in the following.

Figures 3, 4, 5 show the impact of -155 dBW CW interference on the tracking loops, while the worst case GPS L1 C/A PRN 6 code line is impacted. The interference is generated 200 seconds after the beginning of the tracking.

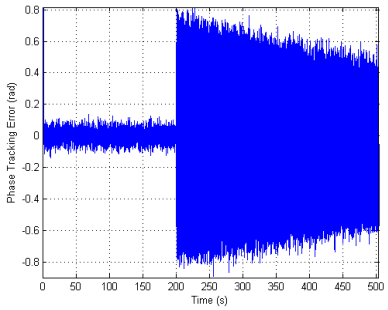

Figure 5 : Phase tracking error with a 10 Hz PLL bandwidth and a dot product discriminator, with CW after 200 seconds simulation.

Here above, a CW was generated after 200 seconds of simulation, to see precisely its impact on the code and phase tracking errors.

The figure represents the phase tracking error when a CW appears 200 seconds after the beginning of the tracking process. It is easy to identify the impact of the interference as sine waves appear on the tracking loops errors. Note also that the interference impacts the two loops.

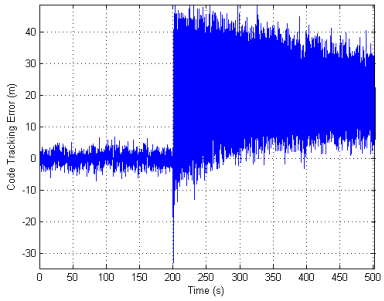

Figure 6 : Code tracking error in a static case with a 1 Hz bandwidth and a dot product discriminator, with CW.

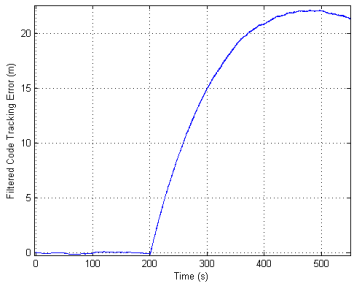

Figure 7 : Code-Carrier error in a static case with a 1 Hz dot product DLL with CW.

Conclusion: CW and NB interference affect the two tracking loops and consequently affect the accuracy of the resulting pseudoranges, and the navigation solution. It is consequently important to be able to detect those perturbations in compliance with APV required accuracy. As the two loops are affected, the code smoothing process will be affected too and the higher the interference power, the higher the resulting pseudorange error. In the case the interference is not detected, it could generate a penalizing error during APV phase of flight without any flag.

III. SIMULATOR SETTINGS: MULTIPLE CORRELATORS , WORST CASE CODE LINES AND JAMMERS

GNSS receivers have several reception channels. Each of them specializes in tracking specific satellites. Each reception channel has at least two or three pairs of correlators (E, L, P) for both code and carrier phase tracking.

A multi correlator receiver can compute much more correlator outputs in a same reception channel. If several correlators are available within a same channel, it is possible to observe the code autocorrelation value in several points spaced by a value denoted *d* in this paper.

In the following, multiple correlators' outputs will be monitored to detect the presence of jammers.

Multiple correlator settings

The correlators spacing *d* and the correlators' window size around the main peak for both GPS and Galileo signals have to be set.

For GPS L1 C/A, assuming the maximum CW frequency is 1.023 MHz, the correlators' window size must be larger than 20.46 chips, it is thus set to 22 chips in our simulations. From the Shannon theory, a maximum correlator spacing of 0.73 chip is required ($F_c<2F_{cw}$), the correlator spacing is thus set to 0.65 chip.

The impact of CW on the correlator outputs for GPS L1 C/A and Galileo E1 signals has the same shape, that is to say a sine wave appears in the autocorrelation. But, as Galileo E1 code spectrum properties are different of GPS L1 C/A (two main lobes between -2MHz and 2MHz appear in the code spectrum which lines are 250 kHz-spaced), an other setting for correlators window size and spacing is required. The maximum correlators spacing being 0.29 chip for the same reasons as GPS L1 C/A, it is set to 0.25 chip. Finally, to comply with the number of correlators used for GPS L1 C/A case, the window size is set to 9 chips.

IV. PROPOSED DETECTION TECHNIQUES ON CORRELATORS' OUTPUTS

Two techniques were considered, presented below.

Computation of the FFT of the correlators' outputs

Multiple correlator outputs are monitored and the presence of interferences in the incoming signal is detected thanks to the computation of the Fourier Transform of the correlators' outputs [Bastide, 2001]. If undesired carrier sine waves are present, for CW interference, a detection flag is set to 1.

The maximum Fourier transform of the signal is compared to threshold. If a significant sine wave is present in the signal, the maximum Fourier transform of the signal is proportional to the magnitude of the wave, and, in the case the threshold is well chosen, this interference will be detected.

Detection is declared when the following condition is reached [Bastide, 2001]:

$$\left|\max\_ fourier_{inst} - mean(\max\_ fourier)\right| \geq threshold \times std(\max\_ fourier)$$

Where :

- $\max\_ fourier_{inst}$ is the maximum of the Fourier transform at a considered instant
- $mean(\max\_ fourier)$ is the mean of maxima of the Fourier transforms during the training stage
- $std(\max\_ fourier)$ is the standard deviation of the maxima of the Fourier transforms during the training stage
- $threshold$ is the chosen threshold for detection

Figure 9 shows the distribution of this test criterion using 1.5 10^5 samples. The detection threshold compliant with APV P_{FA} is plotted thanks to red lines.

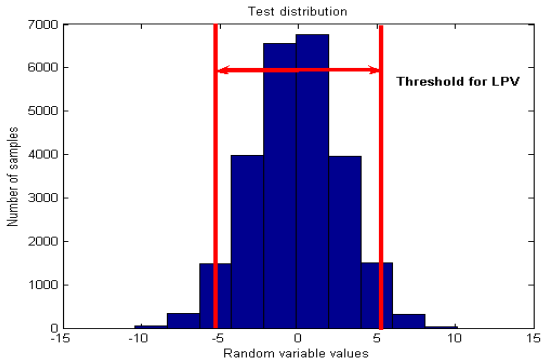

Figure 8 : Gaussian behaviour of the test distribution

One of the interests of this detection principle is that it is based on the maxima of the Fourier transform of the signal and won't detect multipath as those ones will be ignored by the use of sufficiently high detection threshold. Indeed, the presence of multipath is also characterized by peaks on the Fourier transforms of the signals and the computation of the mean and standard deviation of the maxima allows taking into account the low-time variations of multipath. As multipath occurring during flight depends upon the environment (specular or diffuse multipath with different amplitudes), it is interesting to generate multipath in our simulations to know its actual impact during critical phases of flight for instance.

Multichannel Autoregressive model of correlators' outputs

Another algorithm we propose is based on the detection of non regular time variation of an AR model of the set of the correlation outputs. We just provide here a short description of the algorithm and we discuss the main advantages of this algorithm.

We use the correlator outputs noise supposed Gaussian and white.

If a CW or a NB interferes with the incoming signal, then the variance increases exactly when the interference occurs and will vary during the period the signal will be jammed.

A classical AR model could have been used to monitor independently each correlation point, but it is preferable to use a multichannel AR model that will help having a redundant information about all correlators behaviour, on the peak and beside it.

Using this technique, we will exploit the existing correlation between all correlators' outputs in presence of GNSS signals, noise and interferences.

The non-Gaussian behaviour of the time variation of the correlator outputs is also an evidence of the presence of an interferer.

Interferences do not imply a constant additive jump on the correlators' outputs but they imply a time-varying additive jump.

For a first approach, it is not necessary to model the correlators' outputs time-behaviour thanks to an ARMA model.

A short description of the multichannel AR process is provided hereafter.

In the following, x denotes the vector of all the correlators' outputs at the same time epoch. The hermitian property of the model coefficient matrix used for the classical single channel AR model, is not applicable for a multichannel AR model as detailed in [Marple, 1987]. So, the algorithm is a little bit more complex and requires the calculation of forward and backward coefficients (respectively: A and C with corresponding superscripts f and b). We will not describe here all the demonstration of the calculation process, the interested reader should find more details in [Marple, 1987].

Algorithm steps
Initialization
$P_0^f = P_0^b = \frac{1}{N}\sum_{n=1}^{N} x[n]x^H[n]$
$e_0^f[n] = e_0^b[n] = x[n]$
Estimation of the covariance of the residual error for forward, backward and cross
$\hat{P}_p^f = \frac{1}{N}\sum_{n=p+2}^{N} e_p^f[n]e_p^{fH}[n]$
$\hat{P}_p^b = \frac{1}{N}\sum_{n=p+2}^{N} e_p^b[n-1]e_p^{bH}[n-1]$
$\hat{P}_p^{fb} = \frac{1}{N}\sum_{n=p+2}^{N} e_p^f[n]e_p^{bH}[n-1]$
Compute the estimated normalized partial correlation matrix
$\Lambda_{p+1} = (P_p^{f1/2})^{-1}(P_p^{fb})(P_p^{b1/2})^{-H}$
Update forward and backward reflexion coefficients
$A_{p+1}(p+1) = -(P_p^{f1/2})(\Lambda_{p+1})(P_p^{b1/2})^{-1}$
$C_{p+1}(p+1) = -(P_p^{b1/2})(\Lambda_{p+1}^H)(P_p^{f1/2})^{-1}$
Update the forward and backward error covariance
$P_{p+1}^f = (I - A_{p+1}(p+1)C_{p+1}(p+1))P_p^f$
$P_{p+1}^b = (I - C_{p+1}(p+1)A_{p+1}(p+1))P_p^b$
Update the forward and backward predictor coefficients
$e_{p+1}^f[n] = e_p^f[n] + A_{p+1}[p+1]e_p^b[n-1]$
$e_{p+1}^b[n] = e_p^b[n-1] + C_{p+1}[p+1]e_p^f[n]$
Update the residuals

Table 3 : Autoregressive multichannel modelling.

The model residuals are then monitored thanks to the following criterion calculated within a 3-second sliding window:

$$\log \frac{AR\_model\_error\_within\_window}{previously\_estimated\_AR\_model\_error}$$

- The bottom term set the criterion, it is determined through a training simulation without interferences and under the phase of flight conditions as for the FFT algorithm, before the detection tests.
- The top term, that is to say the AR model errors of correlators' outputs estimated during the detection step will be determined at any instant for each test and compared to the errors calculated during the training simulation.

The detection probability on a window is expected to be higher for three reasons:

- the redundant number of measurements at any instant (number of correlators),

- the use of a sliding window (redundancy of detections),
- the number of samples used by detection window, this algorithm being sequential.

V. DETECTION ALGORITHMS PERFORMANCES EVALUATION PROCESS

We recall here in a few lines the performance evaluation methodology used for the previously proposed algorithms.

1. A detection criterion is defined from correlator output characteristics.
2. The detection algorithm is launched using the detection criterion over non-jammed simulated measurements. Detection criterion parameters are set during a training stage without interference under APV phase of flight conditions (dynamics, multipaths…).
3. Varying the criterion threshold, the APV continuity-compliant threshold is chosen when the false alarm rate is lower or equal to P_{FA} ($1.6\ 10^{-5}$ for APV).
4. Then P_{MD} value is determined, generating interferences and using the defined criterion and threshold over a large number of samples (10^5 at less).

The impact of non-detected interferences on tracking error at any time is then discussed.

P_{MD} value must be multiplied by the interference probability of occurrence to compare the performance obtained to the integrity risk (undetectable failure of the specified accuracy).

Unfortunately, the probability of occurrence of interferences can't be estimated to our knowledge. We therefore only provide the probability of missed detection. It is consequently not possible to evaluate the integrity risk; one can only say how this algorithm will alleviate RAIM algorithms that will be used downstream.

VI. SIMULATION OF ACTUAL APPROACH CONDITIONS

Dynamics

A third-order 10 Hz PLL was used in the following simulations. It is characterised by the coefficients K1, K2 and K3 which are defined in [Stephens, 1995] from the product between the PLL filter bandwidth and the time of integration.

The range is assumed to have the following variation:

$$\tau(k+1) = a_0 + a_1 \cdot time(k+1) + \frac{a_2}{2} \cdot time(k+1)^2 + \frac{a_3}{6} \cdot time(k+1)^3,$$

a_0, a_1, a_2, a_0 being the dynamics parameters corresponding respectively to the position of the aircraft, its ground speed, acceleration and jerk and provided by the following mathematical relations:

- $a_0 = \frac{\text{distance}_{\ sat \to airplane}}{c_{light}}$
- $a_1 = \frac{-Doppler}{F_{carrier}}$, Doppler randomly selected between -10 kHz and + 10 kHz
- $a_2 = \sqrt{(horizontal\_acceleration)^2 + (vertical\_acceleration)^2}$ is the aircraft acceleration
- a_3 is the aircraft jerk.

The receiver outputs the raw code and phase tracking errors ε_τ and ε_φ. 100 seconds code-carrier smoothed pseudorange is estimated, corresponding to the smoothing filter parameter used in civil aviation.

Dynamics were generated taking into account the following maximum defined values for all types of manoeuvres:

GROUND SPEED	**800 KT**	**800 KT**
HORIZONTAL ACCELERATION	**0.58 g**	**2.00 g**
VERTICAL ACCELERATION	**0.5 g**	**1.5 g**
TOTAL JERK	**0.25 g/s**	**0.74 g/s**

Table 4: normal manoeuvres on the left side and abnormal on the right side, [MOPS Galileo, 2007].
Where g = 9.81m/s² and Kt are Knots.

Ground speed, acceleration and jerk are linked as derivatives of position and during a flight, those parameters will vary accordingly and will not be constant and maximum all the time. It is all the more true that during aircraft approach, ground speed will significantly and quickly decrease.

Dynamics and interference detection

Dynamics has a non-negligible impact on the tracking loops as explained previously, it is all the more true for abnormal dynamics. As a consequence, if we want to study the impact of non-detected interferences on the tracking loops, it is necessary to take it into account.

Multipath

We discuss here briefly the impact of multipath on tracking and in particular on the correlation peaks which are monitored during our detection process.

If a multipath occurs during the detection process, because of the contribution of the reflected component, the correlation peak will lose its symmetry. In that sense, the detection can be affected, for instance, while computing the FFT of the correlation peak, as a frequency component near the central peak due to multipath may generate a peak in the FFT, that could be interpreted as interference.

The detection will depend upon the characteristics of the multipath, it is expected a high magnitude replica will induce a strong deformation beside the main peak. It is consequently important to take into account multipath as close as possible to multipath in real conditions of an LPV phase of flight.

Multipath is taken into account during the determination of the detection criterion and is generated for all runs.

The model used is the DLR Aeronautical channel model proposed by [Lehner, 2007] and we recall below the main aspects and setting of the model used.

A 10 degree satellite elevation was chosen to perform simulations with worst conditions and the model was launched during the 500 seconds tracking. It corresponds to the elevation mask angle for future Galileo satellites provided by Galileo [MOPS Galileo, 2007]. It is higher than the GPS elevation mask angle which is 5°.

For an in-flight aircraft, it has been demonstrated in [Steingass, 2004] that the wings reflection power level is very low, so it is not considered in the model. Only the fuselage and ground reflections are taken into account.

As shown in [Steingass, 2004], a quite strong reflection close to the direct signal was identified, when analyzing the impulse response of the high resolution aeronautical channel model. It is one to two nanoseconds delayed from the direct path. This reflection has been identified and located near the antenna, on the aircraft fuselage. It was called fuselage echo. The power of this echo is estimated to -14.2 dB. Consequently, the multipath model will be composed of a ground reflection, a fuselage reflection and echo.

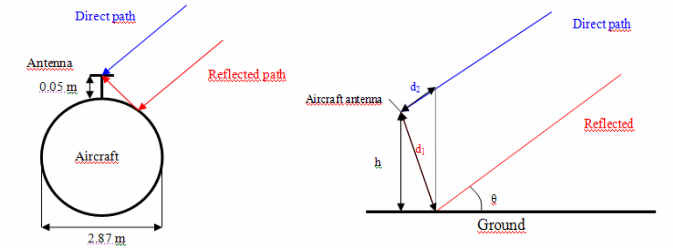

Figure 9 : fuselage and ground generated multipaths schemes.

The correlator outputs are affected by multipath, affecting in trn code and phase tracking errors, respectively ε_τ and ε_θ. The multipath parameters are:

- α1, α2, α3, respectively the relative amplitudes of the ground echo, the fuselage refracted signal and the fuselage reflected signal.
- Δτ1, Δτ2, Δτ3, the code delays of the ground echo, the fuselage refracted signal and the fuselage reflected signal.
- $\Delta\theta 1$, $\Delta\theta 2$, $\Delta\theta 3$, the relative phase shifts of the carrier of the ground echo, the fuselage refracted signal and the fuselage reflected signal.

Correlator outputs models used in the simulator are only valid if the multipath parameters do not vary very fast compared to the integration time.

Multipath and interference detection

As the detection algorithms proposed are based on the monitoring of the correlators' outputs, it is necessary to take into account the impact of multipaths on it. Indeed, due to multipaths, a deformation of the correlation peak may be flagged as an interference while computing the FFT or looking at the temporal variations of a correlation point near the peak.

The model used here simulates multipaths on the Graz Airport (Austria) where empirical tests were conducted to set the model. It is obvious that multipath impact on the correlator outputs will be dependant upon the targeted airport geometry.

VII. PMD ESTIMATION AND UNDETECTED PSEUDORANGE ERRORS INDUCED

The obtained P_{MD} value for the worst case CW (-155 dBW) for GPS L1 C/A signal, is 6.7 10^{-5} using the snapshot FFT algorithm. On the next figures are represented the maximum raw and smoothed code tracking error values undetected by this algorithm for different interference amplitudes and considering different PRN. The smoothed code error never exceeds 15 meters in the GPS case.

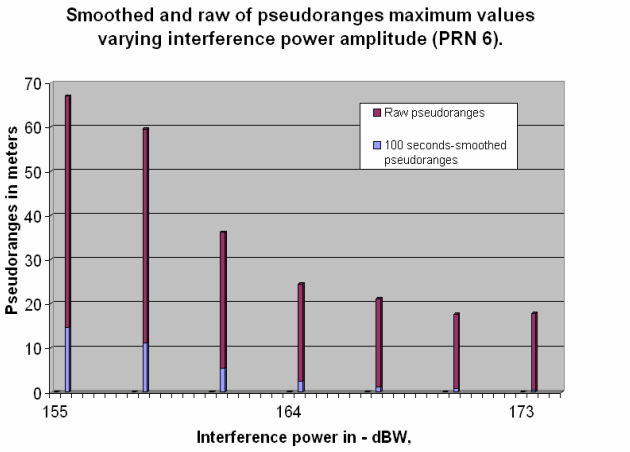

Figure 10 : amplitude of tracking errors as a function of interference power resulting from non-detected CW on the GPS L1 C/A code, PRN 6.

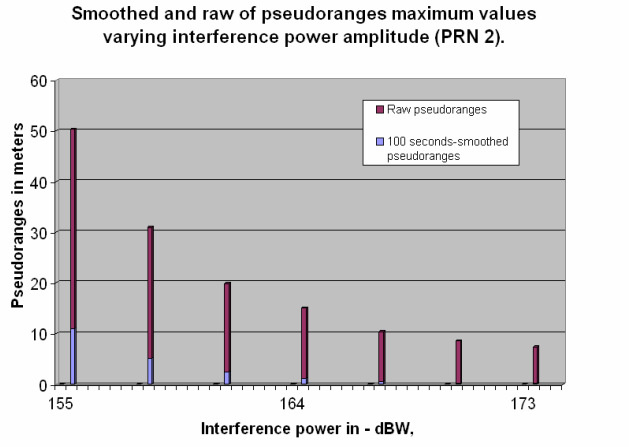

Figure 11 : amplitude of tracking errors as a function of interference power resulting from non-detected CW on the GPS L1 C/A code, PRN 2.

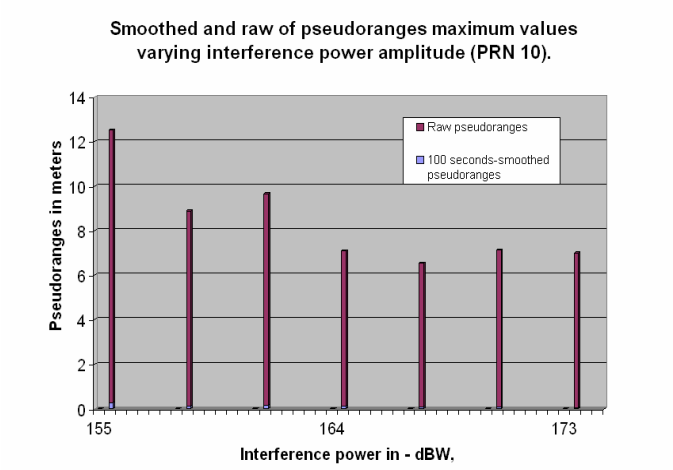

Figure 12 : amplitude of tracking errors as a function of interference power resulting from non-detected CW on the GPS L1 C/A code, PRN 10.

The obtained P_{MD} value for the worst case CW for Galileo E1 signal is below 10^{-5}. Hereafter is represented the maximum raw and smoothed code tracking errors obtained for undetected CW, varying the amplitude value. The smoothed error never exceeds 2 meters.

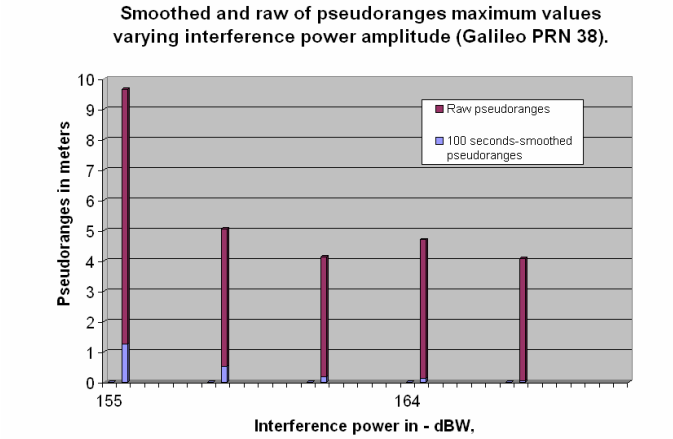

Figure 13 : amplitude of tracking errors as a function of interference power resulting from non-detected CW on the Galileo E1 code, PRN 38.

For NBI cases, tests results will be presented in other reports.

P_{MD} obtained for both worst case CW and NB using the multichannel AR model with a 3s-time detection window are comparable to the P_{MD} obtained thanks to the FFT algorithm. But, this AR algorithm needs to be tested with different settings (width of the detection window, number of correlators).

VIII. DISCUSSION OF OBTAINED RESULTS

A first remark is that if one wants to implement the FFT detection technique or the AR one within future receivers, the detection criteria parameters and thresholds under actual normal aircraft conditions of dynamics and multipath have to be previously saved.

As shown in figure 8, jammers impact on the correlator outputs differs with the amplitude of the interference, indeed, the more the amplitude of the interference, the more the amplitude of the sine wave. The two techniques have different approaches, considering the instantaneous behaviour of the correlators outputs in the Fourier domain or considering the time evolution of those ones.

The highest missed detection probabilities were obtained for high amplitude interferences (worst case for a CW: -155 dBW) and worst case code spectrum lines. It seems that for Galileo signal case see (PRN 38), the maximum smoothing error generated by an undetected interference is smaller than for GPS L1 C/A, this is due to the fact Galileo code spectrum lines have a lower amplitude than GPS L1 C/A ones.

It can be also clearly seen that the impact of CW on the worst case code lines in terms of raw pseudorange errors is larger than for other lines as PRN 10 worst case code line for instance.

Discussion about the proposed detection algorithms and civil aviation requirements

Concerning the first snapshot algorithm, the choice of the criterion calculating the maximum of the Fourier transform, allows reducing the impact of low power multipath (like echoes on the aircraft fuselage).

The AR algorithm allows taking into account simultaneous variations of all correlators' outputs, it consequently decreases the P_{MD}.

Below are recalled civil aviation requirements for NPA and APV phases of flight in terms of accuracy and integrity. TTA stands for Time To Alert, it is the maximum allowable time interval between system performance ceasing to meet operational performance limits and the appropriate integrity monitoring subsystem providing an alert.

	NPA	APV I	APV II
Accuracy hor.	220 m	16 m	TBD
Accuracy ver.	x	8 m	TBD
Integrity	10^{-7}/h	2.10^{-7}/app	2.10^{-7}/app
TTA	10 sec	10 sec	6 sec
P_{FA}	$3.33.10^{-7}$	$1.6.10^{-5}$	TBD

Table 5 : Civil Aviation requirements [DO229D, 2006].

It is important to obtain a low time of detection with regards to TTA to maintain integrity. That is why a short time detection sliding window (3 seconds) was chosen for the AR model taking into account APV TTA, the FFT algorithm being snapshot.

For each phase of flight, to ensure that the position error is acceptable, alert limits are defined and represent the largest position error which results in a safe operation.

P_{MD} value obtained during our simulations must be multiplied by the interference probability of occurrence to compare to the integrity risk (undetectable failure of the specified accuracy) requirement.

Unfortunately, the probability of occurrence of interferences can't be estimated to our knowledge. It is consequently not possible to evaluate the integrity risk; one can

only say how this algorithm will alleviate RAIM algorithms that will be used downstream and will be useful to launch repair algorithms or to switch to other GNSS components available during the RFI crossing to maintain the level of performance required during the phase of flight as described in [Mabilleau, 2007].

IX. CONCLUSION AND FUTURE WORKS

In our simulations, worst cases were considered in terms of interference power, code spectrum lines impacted, which makes our P_{MD} estimation robust against the mentioned interferences.

Each interference was generated using a Doppler variation rate (between code lines and interference) of 2Hz/s for each tracking trial. So, interferences not always stroke exactly the worst spectrum lines.

We did not discuss the impact of abnormal dynamics here, so a special care must be taken in this case as it is important to know the resulting errors and the integrity risk induced by this event.

Two algorithms were proposed a snapshot one (FFT criterion) and a sequential one (AR model).

Such detection algorithms will alleviate and complete the detection made by RAIM-type algorithms (but only for interferences). The obtained P_{MD} are between 10^{-4} and 10^{-5} for the worst case -155 dBW CW. Those results concern each worst case GPS L1 C/A PRN 6 and GALILEO E1 PRN 38 worst case code spectrum lines using each of the two proposed detection algorithms.

The resulting maximum error on smoothed pseudoranges when no detection algorithm is used is around 15 meters for GPS L1 C/A and around 1 meter for Galileo E1.

The presented techniques are consequently useful when an interference occurs during approach phases of flight like APV because, it will allow detecting a degradation due to a CW or a NB with a low P_{MD} (integrity) and in case of failure in the detection, the resulting error will not exceed 1 meter while using Galileo E1 for positioning. This error will not have a harmful impact on the protection level computation in this case.

Those results have to be compared with RAIM detection capabilities.

When detection is made and when there is an impact on performances (accuracy), it is possible to repair data thanks to the characterization of interferences with a Prony-like model for instance. Interference effects should be removed in this case for accuracy purposes.

After detection, the next step consists in two options: using another GNSS component for positioning or removing the incoming interference if possible.

ACKNOWLEDGMENTS

The first author would like to thanks Igor Nikiforov from the Université de Technologie de Troyes (UTT) in France for the interesting discussions he had with him about mathematical models of detection algorithms.

REFERENCES

[Bastide, 2001] *F. Bastide*, GPS interference detection and identification using multicorrelator receivers, ION 2001

[Burnham, 2004] Multimodel Inference: Understanding AIC and BIC in Model selection, *Kenneth P.Burnham, David R. Anderson, Colorado State University, 2004.*

[Esbri, 2006] Antenna-based Multipath and Interference Mitigation for Aeronautical Applications: Present and Future, *O. Esbri-Rodriguez, DLR German Aerospace Center, Germany, M. Philippakis, ERA Technology (Cobham PLC), U.K., A. Konovaltsev, DLR German Aerospace Center, Germany, F. Antreich, DLR German Aerospace Center, Germany, C. Martel, ONERA, France (formerly with ERA Technology (Cobham PLC), U.K.), D. Moore, ERA Technology (Cobham PLC), U.K, 2006.*

[Holmes, 1990] Coherent Spread Spectrum Systems, Holmes, Krieger, 1990.

[Julien, 2005] PhD Thesis: Design of Galileo L1F Receiver Tracking Loops, *Olivier Julien, July 2005.*

[Lehner, 2007] Multipath Channel Modelling for Satellite Navigation Systems, *Andreas Lehner, Shaker Verlag, 2007.*

[Mabilleau, 2007] Combined GALILEO-GPS receiver based on a switching logic, *Mikaël Mabilleau (DTI), Paul Nisner (NATS), Laurent Azoulai (Airbus), Jean Pierre Arenthens (Thales), Gerard Alcouffe (Thales), Christophe Ouzeau (ENAC), Navigation System Panel, New Delhi, India, March 2007.*

[Macabiau, 2006] GNSS Airborne Multipath Errors Distribution Using the High Resolution Aeronautical Channel Model and Comparison to SARPS Error Curve, *Christophe Macabiau, Laetitia Moriella, Mathieu Raimondi, ENAC/INSA, Cyril Dupouy, STNA, Alexander Steingass, Andreas Lehner, DLR, ION NTM 2006.*

[Marple, 1987] Digital Spectral Analysis With Applications, *S. Lawrence Marple*, Jr., Prentice Hall, Signal Processing Series, 1987.

[MOPS Galileo, 2007] Minimum Operational Performance Standards for Galileo, EUROCAE, WG 62, 2007.

[Raimondi, 2006] Mitigating Pulsed Interference Using Frequency Domain Adaptive Filtering, *Mathieu Raimondi, ENAC/INSA, Christophe Macabiau, ENAC, Frederic Bastide, Sofreavia/DTI, Olivier Julien, ENAC, ION GNSS 2006.*

[DO229D, 2006] Minimum Operational Performance Standards For Global Positioning System/ Wide Area Augmentation System Airborne Equipment, RTCA Paper No. 093-06/SC-159-939, 2006.

[DO235A, 2002] Assessment of Radio Frequency Interference Relevant to the GNSS, DO-235A, RTCA SC-159 Inc, 2002.

[Steingass, 2004] The High Resolution Aeronautical Multipath Navigation Channel, *Alexander Steingass, German Aerospace Center DLR, Andreas Lehner, German Aerospace Center DLR, Fernando Pérez-Fontán, University of Vigo, Spain, Erwin Kubista, Joanneum Research, Austria, Maria Jesús Martín, University of Vigo, Spain and Bertram Arbesser-Rastburg, European Space Agency, The Netherlands, ION 2004.*

[Stephens, 1995] *S. A. Stephens, J. B. Thomas*, "Controlled-Root Formulation For Digital Phase-Locked Loops".